Foaming Mechanism Characterization in Cathode Ray Tube Glass Foams

By

Joshua Pritchard

&

Andres Garcia

A Thesis

Submitted to the Faculty of the

N.Y.S. College of Ceramics at Alfred University

in Partial Fulfillment of the Requirements

for the Degree of

Bachelor of Science in Material Science & Engineering

Thesis Advisor: Dr. Anthony Wren

May 5, 2016

Acknowledgements

We wish to express our sincere gratitude to Dr. Anthony Wren for taking us on as thesis students halfway through the academic year. Our thesis advisor of the first semester left and we were without guidance.

We sincerely thank graduate student Yuxuan Gong for guiding us through parts of our experimental process and assisting us in deciding the scope of our thesis along with its goals.

I, Joshua, would like to personally thank my co-worker and Boston University professor Zlatko Vasilkoski. He assisted me with the MATLAB analysis of our ESEM pictures. I learned a great deal from the entire process and I greatly appreciate all of his spare time that he gave to me.

Table of Contents

Abstract

Waste cathode ray tube (CRT) glass contains hazardous heavy metals, and is often disposed of at landfill sites. This disposal method of waste CRT glass possesses potential impact on the environment of landfill sites given its poor retention of heavy metals. This study uses waste CRT glass in producing fast sintered (~ 600 seconds) and highly porous (from ~ 30% to 90% porosity) glass foams. Redox and thermal decomposition foaming agents were used to prepare glass foams in an attempt to understand the relationship between amounts of released gas and porous structure. Two different types of CRT glass, panel glass and funnel glass, were compared to study the effect of glass composition on porous structure. The waste CRT glass was pulverized, mixed with silicon carbide or calcium carbonate (at a given volume of released gas), pressurized into pellet shape using uniaxial press, and then sintered at 900^{o}C. The as-prepared foam glasses were characterized using Archimedes method, pycnometer, X-ray diffraction (XRD) and scanning electron microscopy (ESEM) to investigate the structural, processing, and composition relationship. Samples foamed using redox foaming method maintained a closed pore structure, and the bulk density decreased with increasing addition of foaming agent; samples foamed by thermal decomposition method displayed open pore structures, and the bulk density increased with increasing addition of foaming agent. All foams made with funnel CRT glass have a lower bulk density comparing to their panel glass counterparts. The porous structure was found to be governed by the gas release rate. The glass foams from redox foaming method showed potential to be used in applications such as shock-wave absorption, sound absorption, and heat retardation.

I. Introduction

Foam glass is currently a relatively small market but it does have many uses which include, but are not limited to, cold and hot insulation works, waterproofing, and noise mitigation works. It is commonly valued for having good general insulating properties and also doubling as a useful structural component. An interesting aspect of glass foam is that it is very reasonable to manufacture from entirely recycled materials. This makes it a potentially cheap and environmentally friendly product. Glass foam can be made from many different compositions of glass and can utilize different recycled foaming agents.

Even though foam glass is not considered exclusively part of one market it is reasonable to say that it, for the most part, belongs to the insulation market. Even though it only holds a fraction of the total market, more and more contractors are learning the uses and advantages of using glass foams over traditional insulations for certain applications. As shown below in Figure 1 the insulation market is growing at a steady pace.

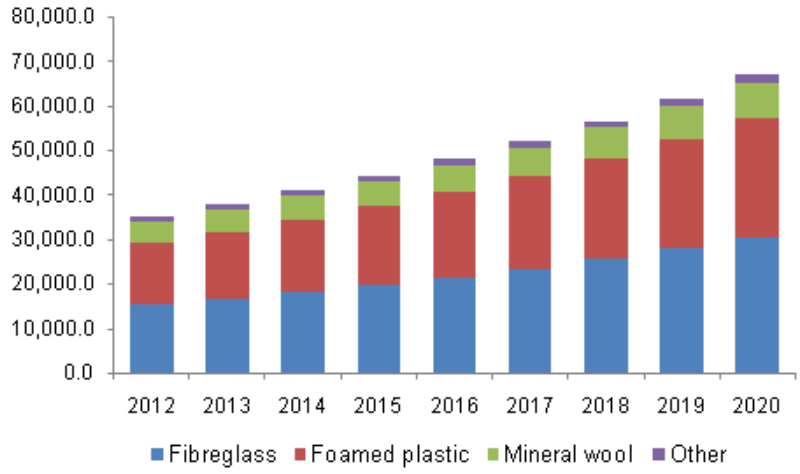

Figure 1. North American insulation market revenue by product in USD Millions. 2012-2020. (Insulation Market Size)

Although glass foams market share only falls into the "other" category, as the entire market grows so will its share. More importantly glass foam is starting to replace some traditional foams, more specifically mineral wools, which could cause its market share to rapidly grow.

Mineral wools are currently industry standard for many extreme temperature piping applications. They can hold up at high and low temperatures; they are "noncombustible" and they have similar thermal expansions and contractions to steel (Pittsburgh Corning). Glass foams share all of these properties and can easily compete with mineral wools in performance. On top of this glass foams are non-wicking, which is something that mineral wools and other comparable products are not. Wicking can be a serious problem in high temperature environments where the insulation could possibly absorb combustible liquids such as oils, heat transfer fluids, resins, solvents, or silicones (Pittsburgh Corning). Build-up of these combustibles can then auto-ignite when exposed to more oxygen in situations like repairs (Pittsburgh Corning). An example of a wicking experiment is shown below where the glass foam is the only material not to absorb the combustible. For this safety reason glass foam insulations are starting to replace mineral wools in various high temp applications.

Figure 2. Foam glass insulation (right) demonstrates no wicking or combustion while mineral wool, calcium silicate and two different brands of perlite sustain flames from wicking of oil (Pittsburgh Corning)

Sticking with insulation applications, glass foam is also very chemically resistant for insulation. This derives from the naturally high chemical resistance of glass; glass foam also has no binders or fibers where a chemical attack could readily take place. In the case of closed pore glass foams even successful chemical attacks are segmented and are often limited by accessibility to surfaces. To further this point the chart referenced as Appendix 1 shows how a foam glass product stands up against other polymer foams (Pittsburgh Corning).

Another property that foam glass has that is not typical of most insulating materials is its ability to handle compressive stresses. This property is usually not considered for many insulations as it is so limited. However, for certain applications it can be very useful. For insulating tall silos and long vertical pipes glass foam can easily be used with no additional supports because it can support itself (Pittsburg Corning). This can apply to any buildings needing self-supporting insulation. Glass foam can be very versatile and useful as a structural component in construction.

Most glass foams are only made out of two raw materials: the glass and the foaming agent. The raw glass can be remarkably different and yet obtain similar goals, however it can have some unintended consequences. This is on a case by case basis depending on the composition as different foaming agents can provide drastically different results. There are two main types of foaming agents. The first types are foaming agents that decompose and release gas under heat, due to thermal decomposition. These include compounds like $CaCO_3$ and other oxides. The chemical reaction for Calcium Carbonate to Calcium Oxide and Carbon Dioxide is shown below.

$CaCO_3(s) \rightarrow CaO(s) + CO_2(g)$

Degassing foaming agents like this will usually result in open porosity foam. Thermal decomposition processes are preferable for glass containing high amounts of heavy metals, since they do not present the risk of oxidation reactions by the reduction of easily reducible oxides, like those of some heavy metals (Bernardo, 2006). The other type of foaming used to make foam glass involves redox reactions that effectively uses the oxygen available from the oxides in the glass structure to form CO_2 or some other gas which can include CO and O_2. A very common form of this method involves SiC. There is more than one reaction that this process depends on. One of these reactions is shown below.

$SiC(s) + 2O_2(g) \rightarrow SiO_2(s) + CO_2\ (g)$

This reaction however is slow, even at 900 °C, and is likely not the cause for most of the foaming. It is much more likely to form carbon monoxide (CO) than carbon dioxide (CO_2). The resulting CO^- is reactive with other oxides in the glass, especially those that are easily reducible, like heavy metal oxides. The CO^- strips them of their oxygen to form CO_2 and leaves just the heavy metal behind. SiC can also directly react with other oxides as shown below:

$4PbO\ (s) + SiC\ (s) \longrightarrow Pb\ (s) + SiO_2\ (s) + CO_2\ (g) \uparrow$

Redox reaction foaming will generally result in a much more closed porosity foaming than that of thermal decomposition. Both modes of foaming have their own specific uses along with pros and cons. Having both mechanisms achieved at the same time generally does not give favorable results. There are many factors at play for both foaming mechanisms and they will be discussed at great lengths in this paper.

Regardless of the application albeit insulation, structural support, or chemical barriers, most foam glasses can be formed from entirely recycled products. With all their uses this makes them a very exciting product as we move into a greener future. Researchers have started using all kinds of recycled waste. Waste glass from bottles has commonly been recycled into production (Gong). Materials as extreme as waste glass from CRT TV's have also been used in research to determine if this hazardous waste could be used in the manufacturing of foam glass (König). As far as foaming agents there are plenty of creative ideas. For carbonates the use of egg shells and fish or mammal bones have been documented (Gong). For redox reactions from carbides the use of ash and sawdust has been recorded (Apkaryan). For this study raw compound foaming agents were used. It has already been shown through countless research that recycled materials can be used as foaming agents (Gong; Fernandes). So this decision to use raw compounds was made to limit the number of variables in the presented research.

Environmental Impact of CRT Waste

The impact of waste CRTs is a global environmental issue. The shift from the bulky CRTs to the preferred flat screens of today's TVs and monitors has driven the increasing waste at a much faster rate. Traditional means of recycling are not effective enough to deal with the high levels of toxic heavy metals in the glass, such as lead, barium, and strontium. Incineration is not a viable option due to the plastics containing flame retardants that produce dioxins in the gas mixture (Menad 1999). Disposing in landfills and storage facilities is another option that has been significantly banned in the United States within the past two decades. Common landfills are avoided due to the acidic leaching of the heavy metals into potential ground water. If they were disposed of in a landfill, in the US, the landfills have to be licensed to handle the hazardous wastes although the management costs are constantly increasing (Nnorom 2011).

Despite legislation banning the transportation of hazardous wastes, developed countries in North America and Europe have been reported to transporting their wastes to less developed countries. Even within the developing countries, there are huge movements of the CRTs to other landfills (Poon 2008; Nnorom 2011).

Sakab, a Swedish company has used CRT glass as a fluxing agent to attach heavy metals instead of land or slag. The smelting of CRT glass is preferable to landfilling but too expensive to be properly commercialized (Menad). A big problem with the recycling of CRTs in America is the lack of actual recycling. A paper by Price in 1999 concluded that only 1000 units of the estimated 1.3 million TVs that became obsolete were recycled, in Florida alone (Nnorom).

Literature Review

Foaming Through Thermal Decomposition

Title: Glass foams from dismantled cathode ray tubes; E. Bernardo and F. Albertini,

Bernardo and Albertini (2005) examined the foaming process of $CaCO_3$ in CRT panel glass by varying the wt. % and thermal treatment. The glass was milled to < 25 μm then milled again with added $CaCO_3$ at 3, 5, and 7 wt. %. The mixtures were uniaxially pressed at 40 MPa in a 31 mm diameter cylindrical die. After drying the pellets overnight at 80 °C the pellets were sintered at 725 °C. Previous works revealed the dilatometric softening temperature of the panel glass occurring at 592.8 °C and the thermal decomposition temperature of $CaCO_3$ occurring at approximately 700 °C, thus justifying the use of 725 °C as the chosen temperature. The variation was in the heating rate and holding time from 5 to 20 °C/minutes and from 5 to 30 minutes respectively.

The foams showed open porosity varying slightly from 93% for 5 °C/minutes heating rate, 90% for 10 °C/minutes and 86% for 20 °C/minutes. Crushing strength of all the samples were found to be within the range of 1 to 4 MPa with the strongest samples being the 5 minute holding time and the 20 °C/min heating rate. Comparing the data, it was concluded that fast heating rates caused a correlation to be made between holding time and concentration of foaming agent. The slower treatments allowed the pores to coalesce and weaken the glass structure. Despite the lower densities of the samples, the longer holding times still showed a crushing strength of approximately 1 MPa which is still comparable to commercial foams. Further tests showed a low thermal conductivity, 0.06-0.07 W/m K, that is also comparable to commercial foams.

Foaming Through Redox Reaction

Title: Preparation of high strength foam glass–ceramics from waste cathode ray tube

Guo et al. (2010) studied the effects of reduction from the addition of SiC in CRT glass. The glass was milled and sieved through 200 mesh, mixed with SiC powder that was sieved through 100 mesh. The samples were prepared using 1 to 7 wt. % SiC and were constantly heated at 5 °C/min to a temperature range of 750-850 °C and holding for 30 minutes. DTA results showed SiC reacting with PbO in the glass starting at approximately 600 °C and 830 °C was chosen as the foaming temperature. Mechanical strength testing showed a maximum strength of 24 MPa and 20 MPa for 1 and 7 wt. % SiC, respectively. A minimum strength of 4 MPa was observed using 4 wt. % SiC. Compared to the values obtained from thermal decomposition, the reduction mechanism shows a much greater mechanical strength.

The high mechanical strength is due in part to the crystal phase precipitates that are formed from the reduction of the metal oxides. XRD patterns showed peaks for Pb, Pb_3O_4 and $Al_6Si_2O_{13}$. The chemistry behind the observed precipitates is caused by the redox reaction of 4 PbO and SiC to form Pb crystals, SiO_2 and releasing CO_2. Remaining SiC reacts with any available O_2 to form SiO_2 and more CO_2. Some of the formed Pb crystals also react with O_2 to for Pb_3O_4. The SiO_2 byproducts of SiC have been shown to be in the cristobalite phase.

In this study, foam glasses were fast sintered (~600 s) successfully using a waste material (CRT glass) as the matrix. SiC and $CaCO_3$ were chosen as the two foaming agents to be used with SiC foaming the glass through a redox reaction and $CaCO_3$ foaming the glass through thermal decomposition. The structural and compositional characteristics of the foam glass samples were characterized to investigate the structural, processing, and composition relationship. The end product of this research will hopefully present a promising use of hazardous waste CRT glass and shed some light on the similarities and differences of two different foaming mechanisms.

II. Experimental Procedure

A. Materials and Preparation

CRT panel and funnel glasses were collected from a single TV monitor. For black and white monitors the overall glass composition had a high concentration of lead to help contain the radiation from the electron gun. The panel glass is the glass from the faceplate of the monitor. Since the switch to color monitors, lead was no longer considered a viable option due to the brown tint and has been mostly replaced with barium and strontium. Neither are as effective at shielding from UV and X-ray radiation as lead and so the glass has to be made thicker than its black and white predecessor. The panel has an internal coating with a conductive material and three layers of phosphors in order to achieve the RGB spectrum. The funnel glass is the part behind the panel leading to the electron gun, tucked under the plastic cover. Since it has no effect on the actual display of the monitor, it still has a high lead oxide concentration of approximately 20 wt. %, and therefore still has the dark brown tint and a smaller thickness than the panel. A quick schematic of a CRT is shown below in Fig. 3 to help demonstrate the components used in this study.

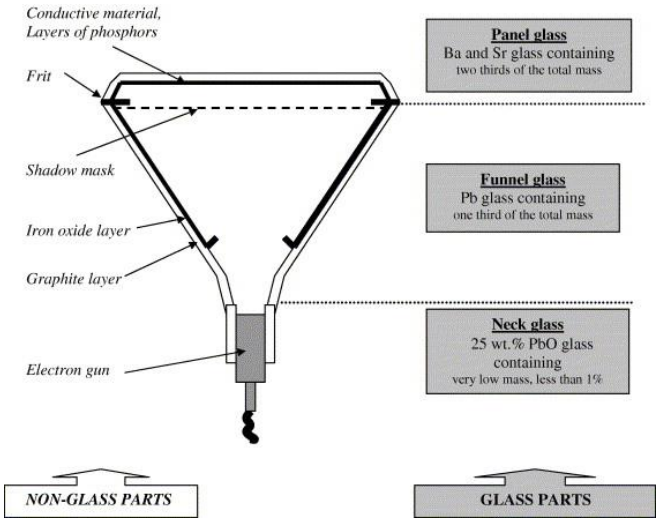

Figure 3. Schematic of typical CRT TV (Méar)

$CaCO_3$ (98.5% purity; Fisher Scientific) was used as the thermal decomposition foaming agent at 5, 10, 15 and 20 wt. %. In order to compare the foaming mechanisms, a normalized CO_2 output was calculated as 2.20, 4.40, 6.60, and 8.80 wt. % by hypothesizing that both foaming agents would fully react. The resulting SiC (Fisher Scientific) used was 2.75, 5.50, 8.25, and 11.00 wt. %. Calculations for the amount of foaming agent are in Appendix 2.

The panel and funnel glass were pulverized into fine particles with a Gyro-Mill (Glen-Creston Ltd., UK) and were respectively sieved to below 45 μm and ball milled with the foaming agents for 3 hours. The powders were pressed into pellets with a one inch stainless steel die with a uniaxial pressure of 35 MPa. The pellets were then placed in a Lindberg Blue M electric furnace and fast heated to 400 °C and held for 600s (to prevent thermal shock) and then 900 °C for 600s (König). The sintered pellets were slow cooled down to 400 °C and then air cooled to room temperature.

B. Phase Identification

X-ray diffraction was performed on the panel and funnel glasses and the sintered pellets with a Bruker D2 Phaser X-ray diffractometer. A Cu kα source with an emission of 10 mA and a voltage of 15 kV was used in measure. The data was collected from 10° to 70° 2θ and compared to that of literature (Méar et al., 2006; Fernandes et al., 2014; Scheffer et al., 2005). The data table shown below is from a previous study (Méar) to help show the approximate values of the metal oxides normally found in CRT glass.

Table 1. Chemical composition [in weight percent] of CRT panel and funnel glass (Méar, 2006)

Oxide	Color panel		Color funnel	
	Range	**Standard content**	**Range**	**Standard content**
Network formers				
SiO_2	60–63	62	52–56	52
Sb_2O_3	0.25–0.5	0.35	0.1–0.3	0.25
As_2O_3	0–0.2	0.02	0–0.1	0.01
Network intermediates				
Al_2O_3	2–3.5	2.2	3.5–5	4
PbO	0–3	–	19–23	22
ZnO	0–0.6	0.3	0–0.1	–
TiO_2	0.4–0.6	0.5	0–0.1	0.05
Network modifiers				
Na_2O	7.8–9	8	6–8	6.8
K_2O	6–7.5	7.5	7.5–8.5	7.8
Li_2O	0–0.5	0.2	0–0.1	–
CaO	0–2	0.5	2–4	3.8
MgO	0–1	0.2	1.2–2	1.8
Fe_2O_3	0.07–0.12	0.08	0.05–0.07	0.06
SrO	6–10	8.5	0–1	0.5
BaO	9–11	10	0–2	1t
CeO_2	0.2–0.3	0.25	–	–
ZrO_2	0–2.5	1.5	–	–

C. Microstructural Characterization

To evaluate the porosity and density of the samples, the glass powder and as-prepared powder density were measured using a helium pycnometer (Micrometrics AccuPyc II 1340 Gas Pycnometer). The bulk density was measured using Archimedes' method (König et al., 2014). Using Eq. (1) the collected densities the total, closed, and open porosity were evaluated.

$$\text{Total Porosity [\%]} = \left(1 - \frac{\rho_{\text{skeletal}}}{\rho_{\text{bulk}}}\right) * 100\% \quad (1)$$

Fractured foam glass samples were imaged using an Environmental Scanning Electron Microscope (ESEM, Quanta 200, Philips-FEI corp., Netherlands). The ESEM was operated at low vacuum with an accelerating voltage of 15 kV. Backscattered electron (BSE) images were used for best showing the contrast based on molecular composition. The selected images were used to calculate the pore size distribution and surface porosity [%]. This was achieved by using a custom MATLAB tool that read the grayscale image and then would enhance the contrast of the grayscale using a contrast-limited adaptive histogram equalization. After this it would attempt to remove the noise using a low-pass filter utilizing the Wiener method. Segmentation of the image would then proceed by implementing an adaptive threshold. The algorithm would attempt to remove all possible holes and small debris which would then only leave circular pores. After segmentation the Watershed algorithms used to isolate the pores. Before this the distance transform of the complement of the binary image needs to be calculated and then pixels that don't belong are set to negative infinity. Then the Watershed algorithm is implemented to find the diameter of all Watershed regions (Meyer). After this is only a matter of looping over the regions to build data set. R-script was then used to organize the dataset into intended outputs.

III. Results & Discussion

A. Microstructural Characterization

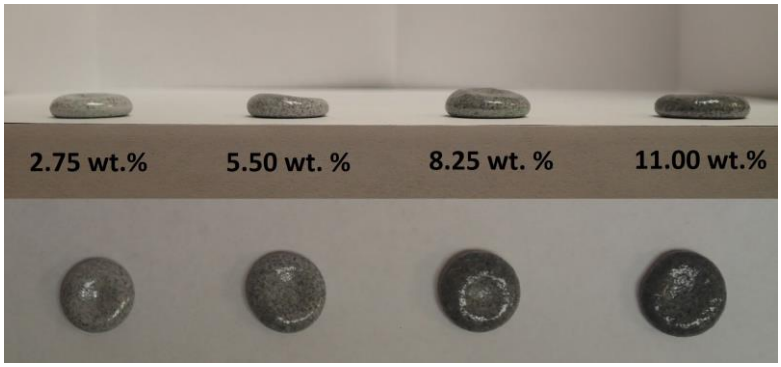

Figure 4. Top and side profile of sintered panel glass with added SiC

As the amount of SiC was increased the samples foamed out more laterally and slightly vertically. Generally the samples were slightly concave in the center. It is apparent from the figures above that not all the SiC was used and caused the samples to darken. All samples had a glassy surface and showed little to no signs of open porosity.

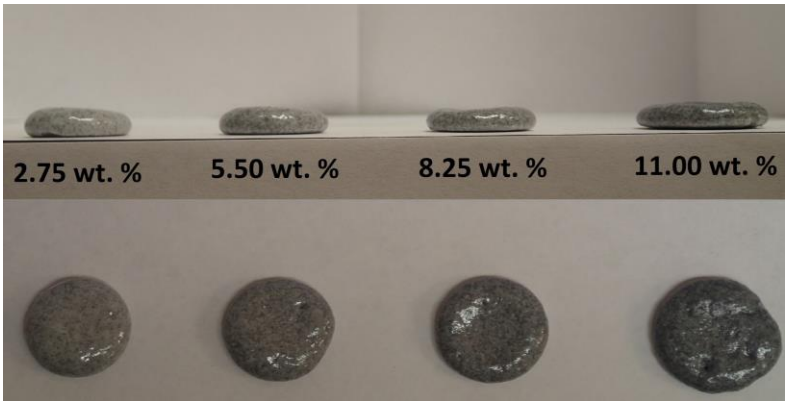

Figure 5. Top and side profile of sintered funnel glass with added SiC

The funnel glass with SiC samples remained more uniform in thickness than the panel glass samples and had a greater lateral expansion. The odd shape of the 8.8 wt.% sample was due to a crack in the pressed pellet pre-sintering. Upon heat treatment, however, the cracks sintered to a close and left noticeable holes from the gas. As with the panel glass, the higher concentration of SiC caused greater expansion and showed a darker color.

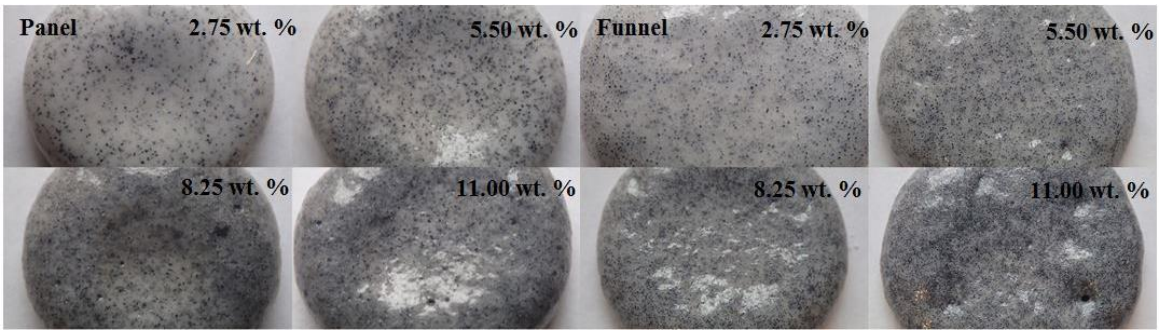

Figure 6. Close ups of all SiC samples

As stated before the funnel samples tended to foam more uniformly and maintain the same thickness throughout the sample. When comparing the panel glass samples to the funnel glass samples the first and most obvious distinction between them is the fact that the funnel glass samples are larger than the panel glass samples. With all of the samples starting with approximately the same volume this would seem to indicate that more gas was released in the funnel samples causing more foaming. This is numerically shown later in this paper with calculated bulk density values. As far as where this extra gas came from is a point of contemplation. It is possible that it was easier for the SiC to react with the funnel glass and create more gas, however it does appear that samples of the same weight percent maintained very similar darkening from present SiC. This is a very qualitative observation so we can't draw conclusions with just these images. Another possibility is that there was already something present in the funnel glass that caused more foaming through a different mechanism, separate of the SiC. This is a topic that will continue to be built on as we progress through the paper.

Figure 7. Side and top view of CaCO3 in panel glass

Figure 8. Close up views of individual pieces

For these samples foamed with $CaCO_3$ it is inconclusive if the funnel samples foamed more than the panel samples as it varied from composition to composition. This may derive from the fact that the structure of these produced foams was by nature very random. Where it was relatively possible to predict what a SiC sample would come out looking like it was much more difficult for these $CaCO_3$ foamed samples. Even though the shapes of these samples where fairly random there still was a general trend observed with the amount of foaming. This trend is opposite from the SiC samples in that the volumes generally decreased as the amount of foaming agent was increased. Through simple visual examination of these samples a hypothesis was formed that, for the samples with less foaming agent present, the gas was not released fast enough to break surface tension as much in the softened glass as it could when more foaming agent was present. The faster and higher volume gas release in the higher composition samples quickly created pathways for gas to escape causing less overall foaming. Of course this is just a hypothesis from nothing more than visual inspection and will be grown upon more throughout the paper. It is also interesting to note that the samples came out white. This is believed to be caused by the excess Calcium left over from the thermal decomposition.

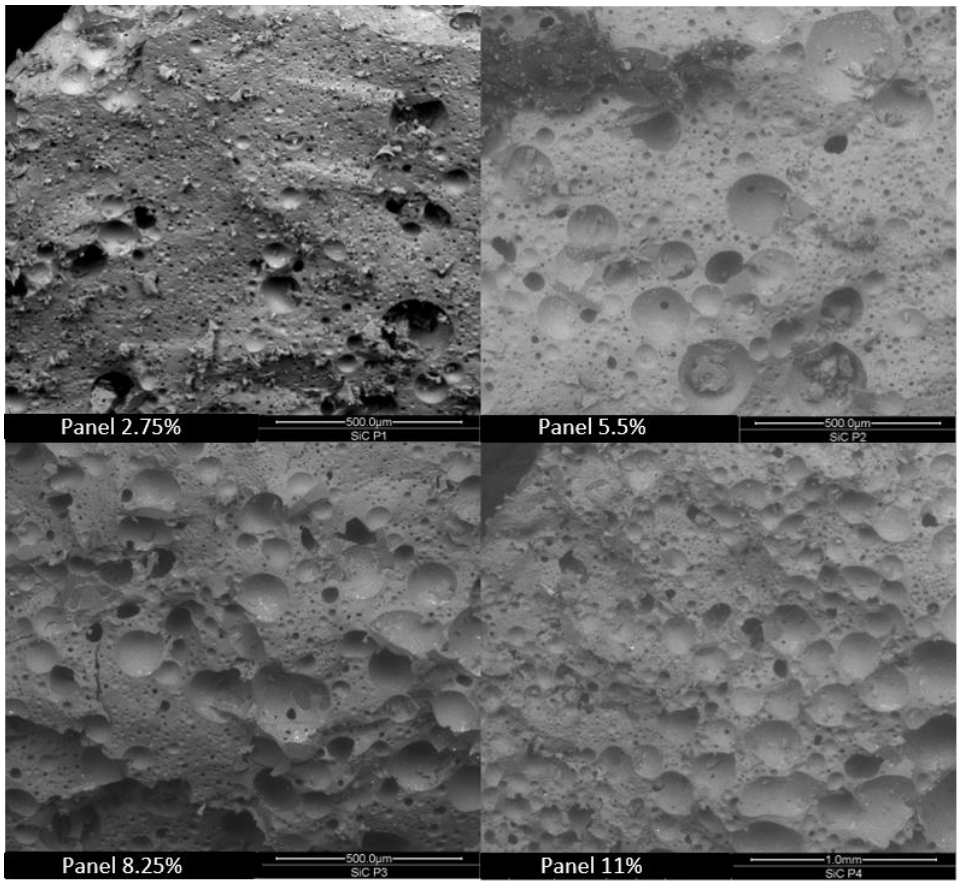

Figure 9. ESEM pictures of SiC Panel samples at various percent compositions

The pictures above depict SiC foam glasses made from panel glass. These foams demonstrate increasing pore size as the percent mass of foaming agent is increased; note that the scale on the bottom right picture is larger than the other images. It is important to note that the pore sizes wildly vary in sizes. Wherever the macropores (greater than 50µm) are not present the volume of the glass is filled with many mesopores (2µm - 50µm), with a large number of them being on the small side of that range. In these foams not many pores are observed to share walls or be in direct contact, which leads to a majority closed porosity. This could mean that this glass had a higher surface tension when softened for foaming causing all of the pores to be absorbed into each other through the process. Note that the 5.5% image has a large darker cluster of material; through examination of other images it has been determined that it is likely contamination. However, it is possible that it is glass that has been stripped of its heavy metals causing it to appear darker on the BSE.

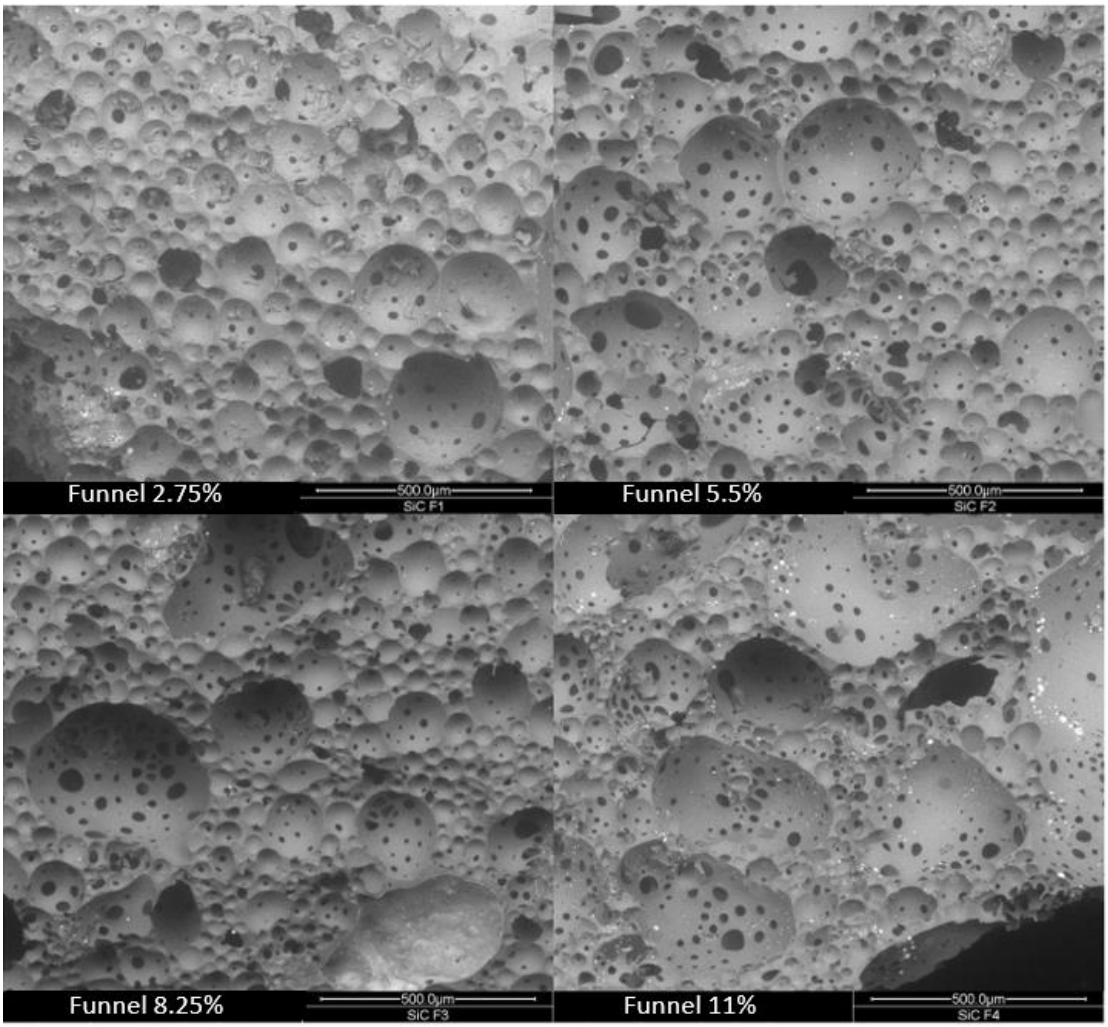

Figure 10. ESEM pictures of SiC Funnel samples at various percent compositions

The pictures above depict SiC foam glasses made from funnel glass. These foams demonstrate increased foaming as the percent mass of foaming agent is increased. The pore sizes in these images vary but not nearly as drastically as the panel. Most of the pores shown above are on the large side of mesopores with many macropores mixed in. In these foams made with funnel glass almost every pore you see is contacting another pore, which leads to a much more open porosity than any of the panel samples along with relatively more uniform microstructure as far as pore distribution is concerned. This could mean that this glass had a lower surface tension when softened for foaming allowing the pores to not draw together.

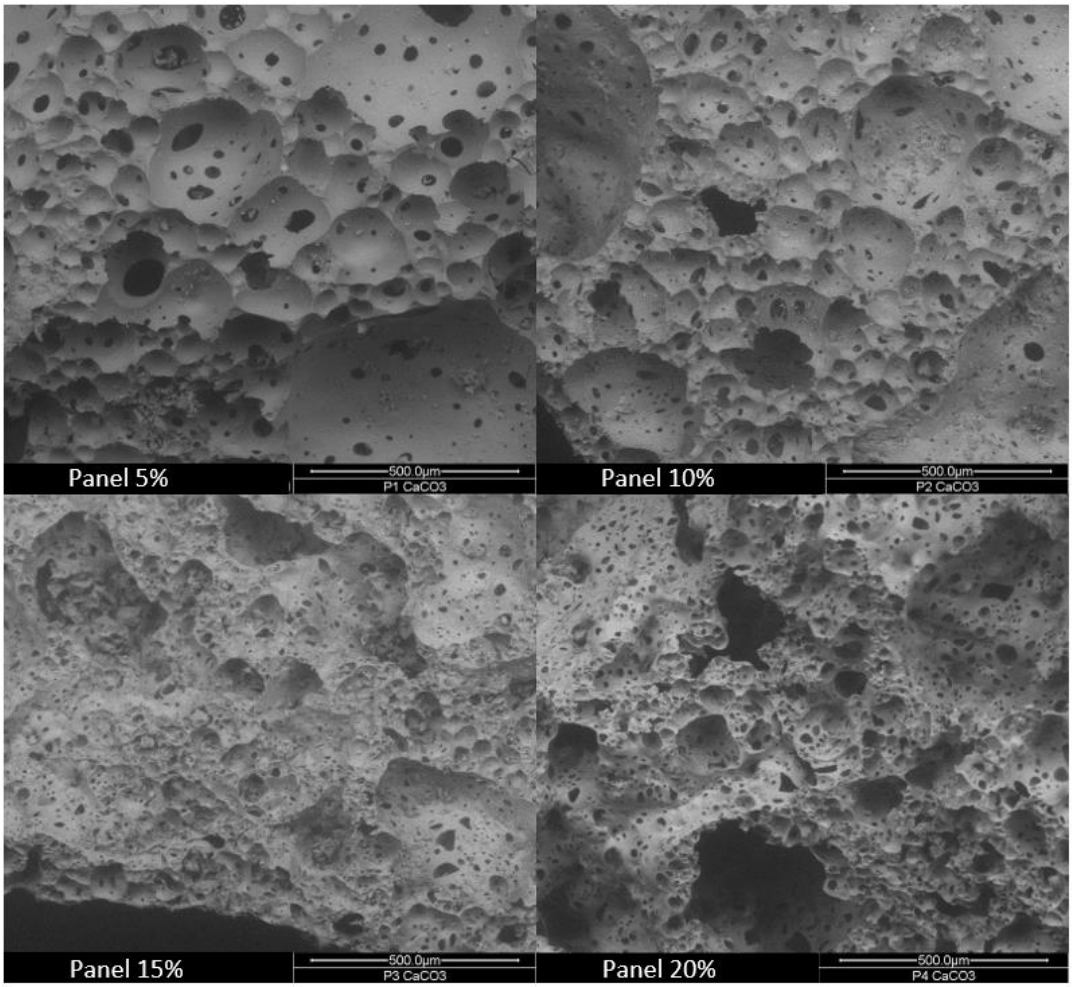

Figure 11. ESEM pictures of CaCO3 Panel samples at various percent compositions

The pictures above depict $CaCO_3$ foam glasses made from Panel glass. Foaming of the samples decreased as the percent mass of foaming agent was increased. The foaming mechanism from $CaCO_3$ is very different than that of SiC. Even the structure of the 5% sample had any significant signs of a typical porous structure with any type of continuity in pore distribution already not present. By the time the weight percent is up to 15% the structure loses almost all features of a typical porous structure and becomes a random structure with large voids. This is caused by too much gas getting released too quickly. $CaCO_3$ decomposes much faster than SiC react so the higher percent compositions the more the gas forces an open and random microstructure, even by amorphous glass foam standards.

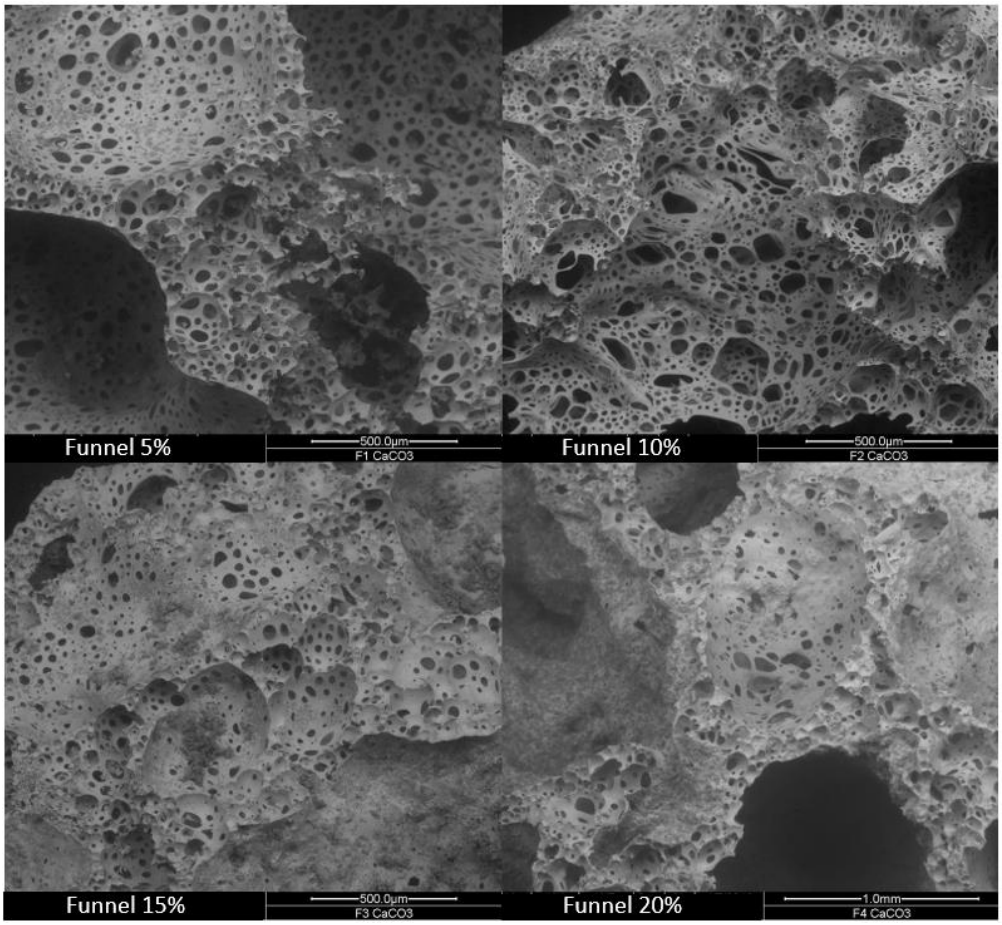

Figure 12. ESEM pictures of CaCO3 Funnel samples at various percent compositions

The pictures above depict $CaCO_3$ foam glasses made from funnel glass. These samples also decreased foaming as the percent mass of foaming agent is increased. The foaming from the funnel glass is even more sporadic than the panel glass which could be caused by the glass being more viscous at the time of foaming or more gas being released during foaming.

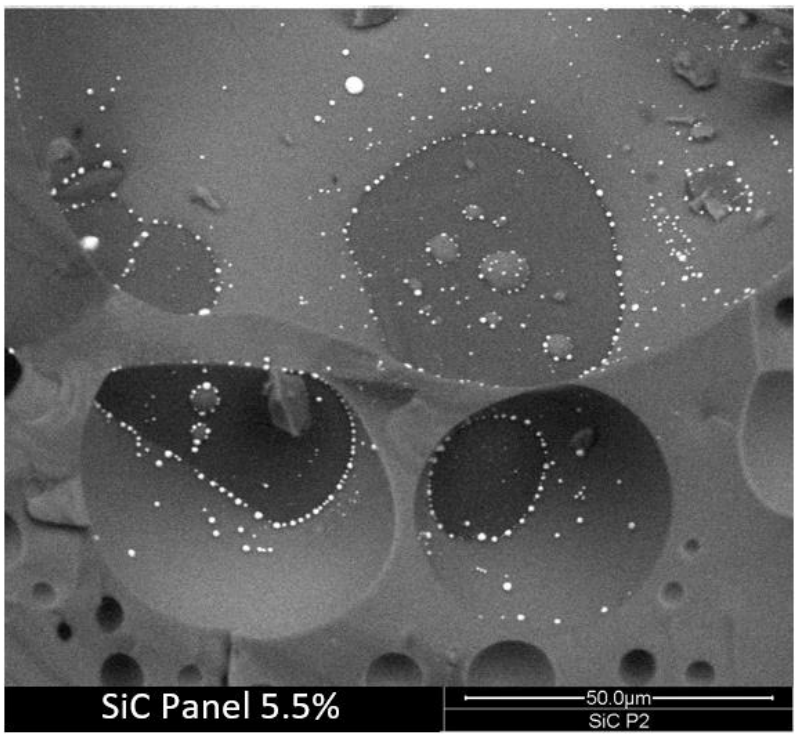

Figure 13. ESEM backscattered picture of panel glass foamed with 5.5% SiC

For this picture note the 50 µm scale, this picture is a close up of a couple interesting pores in a sample. One can see that there are white dots all over the surface of the glass. These dots are metals that have been reduced from the oxides in the glass. This is a panel glass sample so they could be made up of Barium and Strontium but they could also be composed of various different metals in the glass or many combinations. More testing would have to be done to know precisely what metal is being found here. Other than the dots of metals one would also notice darker flat areas that the glass is melted against. All that that one can certainly say from that observation is that the darker area is made of elements with lower atomic masses, as this is a backscattered image. We can however try to draw more hypotheses from it. It has been argued that the dark areas are simply other glass surfaces that have been stripped of the heavier oxides in the glass causing them to appear darker. The researchers, however, in this instance think that the glass is melted up against a piece of SiC that was left in the glass after foaming. One thing to support this argument is that the dark surface appears very flat and uniform like a crystal. Another supporting factor would be that no pore surfaces have observable darkened surfaces due to missing oxides; this is a fairly rare observed feature.

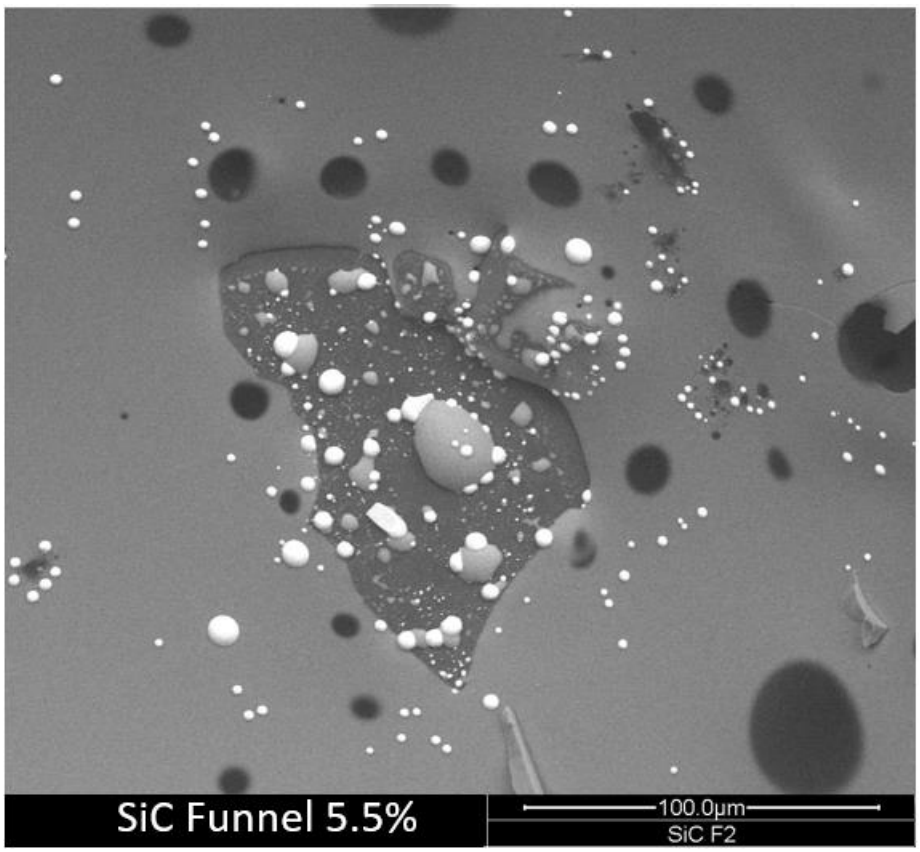

Figure 14. ESEM backscattered picture of funnel glass foamed with 5.5% SiC

In this image, which has a 100 µm scale, one can also observe small dots of heavy metal. There is even more than was observable in the panel glass. This is likely due to all of the lead oxide in the glass that is easily reducible, allowing for more foaming and more metal being separated from the amorphous structure. The metal and glass is seem to be grouping on a piece of what is likely silicon carbide. The glass appears to have a very low contact angle with the surface which would support the idea of a lower surface tension in melt for the funnel glass. An interesting thing to note is that for every bright piece of metal observed in photos it is always grouped up in some way and it almost looks like it recondensed onto the surface of the glass pores. This is because most heavy metals, when in their oxide form, will volatilize when separated from their oxygen before recondensing. This caused the metals found on the surfaces of the pores to be grouped up into droplets.

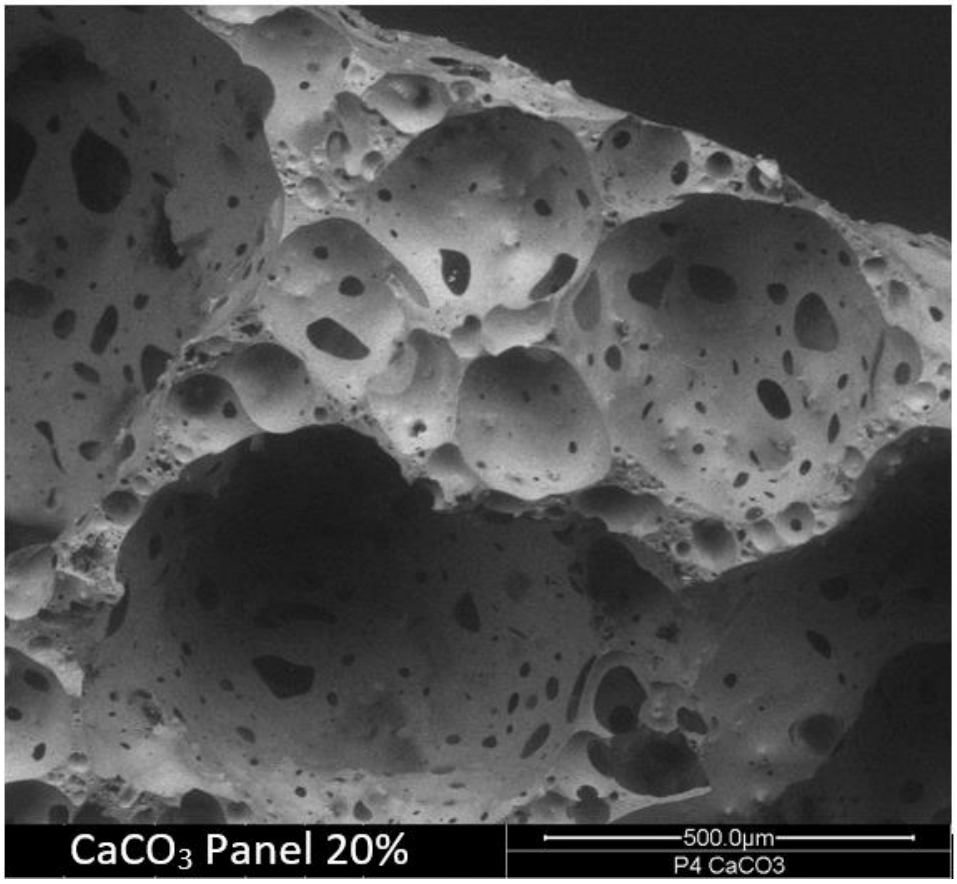

Figure 15. ESEM backscattered picture of panel glass foamed with 20% CaCO3

The effect of the $CaCO_3$ thermal decomposition in the CRT glass matrix is shown to form a great distribution of pore sizes and make the pore walls extremely thin if not properly controlled. Having such thin walls would correlate with lower strength values than those of redox reaction. As shown in Figure 15 the glass foam has no set crystalline structure. Even the walls separating the bigger pores have a porous structure. The top right corner of the figure shows pores breaking the surface of the glass and others still pushing the glass outwards. This process of thermal decomposition can be seen as a direct derivative of the original foaming method through fining glass melts. A major side effect of this process is the lack of uniform structure when looking at the samples as whole.

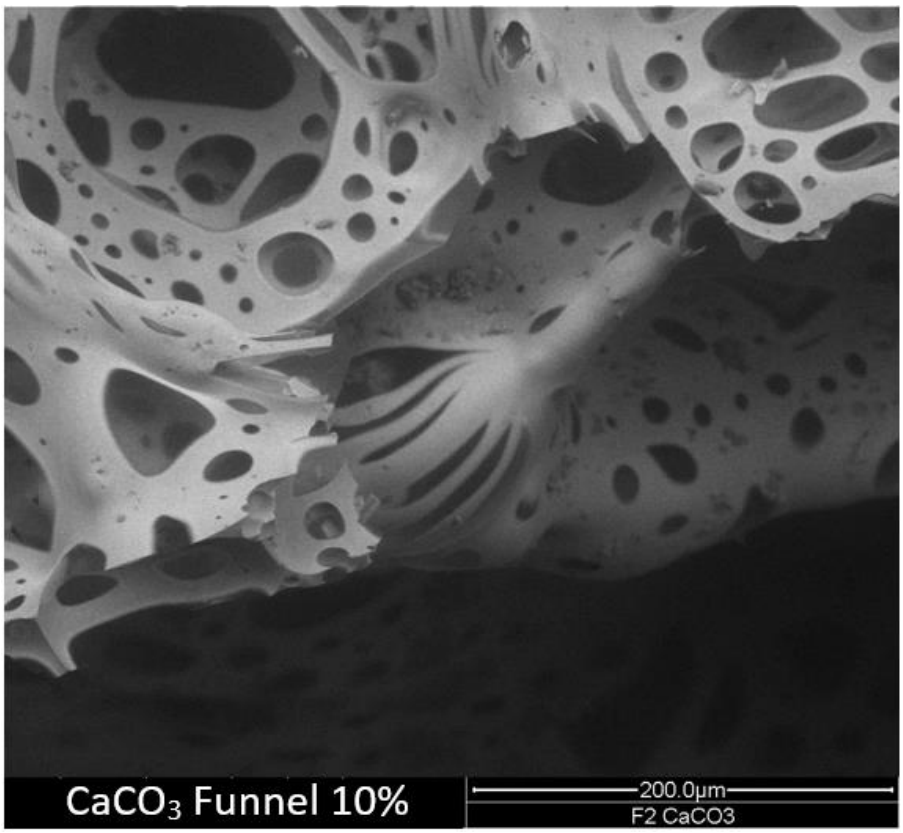

Figure 16. ESEM backscattered picture of funnel glass foamed with 10% CaCO3

A closer magnification of the sintered foam glass at the edge of one of the bigger pores greatly reveals the porous matrix along with any unusual artifacts. As seen in the middle of Figure 16, there appears to be a gill-like structure from what can be speculated to be a pore surface breaking. Within that pore, and just above it, there are some unreacted $CaCO_3$. From observing the rest of the foam structure in the figure the thickness of the walls can be seen to be on the order of microns.

MATLAB Analysis

Selected images of SiC were used to calculate the pore size distribution and surface porosity [%]. An example of a processed image is shown below. Many images were processed like this for each type of SiC sample. The analysis was not applicable on the $CaCO_3$ images as their topography was too extreme.

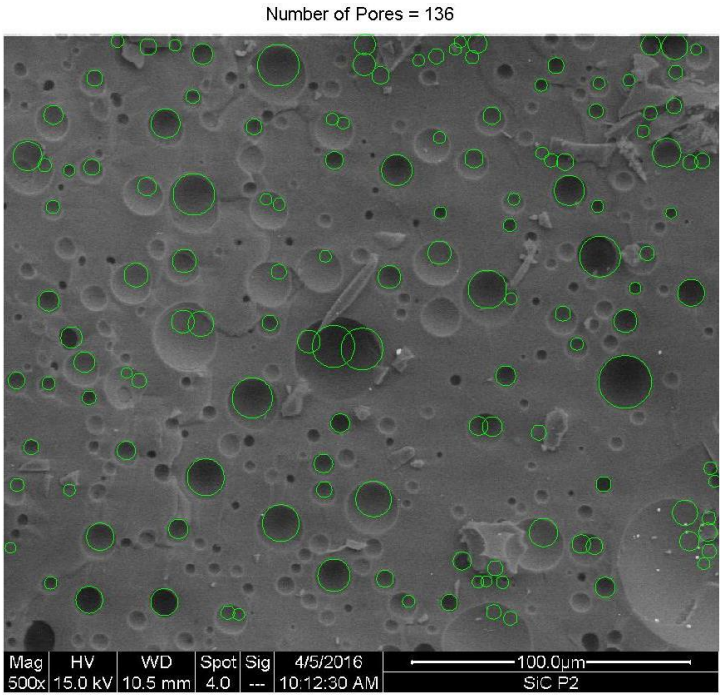

Figure 17. ESEM pictures panel glass foamed with 5.5% SiC. Watershed Algorithm was ran on image to count and measure pores

As you can see above the algorithm is not perfect. Sometimes it fills large pores with multiple small measurements. In other instances the algorithm does not recognize pore, especially small ones. This inaccuracy is a large reason not all results for this technique are presented. The results with much larger datasets provided the most reasonable results. Using this technique was meant to be more of a proof of concept and could be drastically improved upon for future use.

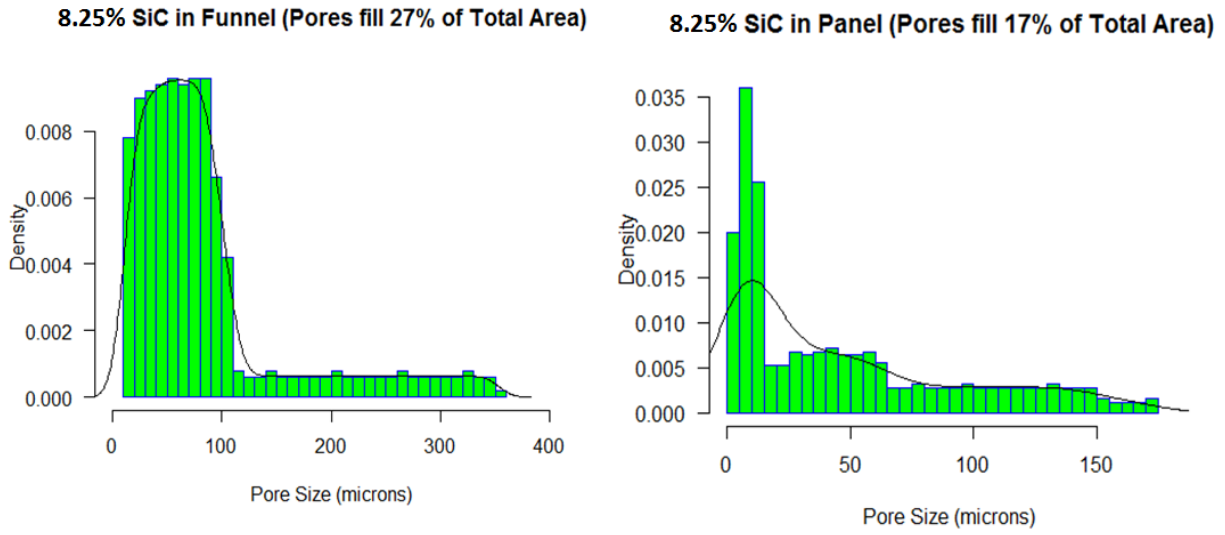

Figure 18. Data for above graphics was calculated using a MATLAB algorithm to detect pores and then R-script to visualize the data

These two graphs represent the pore size distributions for 8.25% SiC glass foam. The left graph is with funnel glass and the right graph is with panel glass. The final product of this analysis was not very accurate to reality when comparing results to the mechanical testing and other studies. The % Porosity provided through this technique was far too low because the algorithm simply missed a reasonable amount of pores in most images. The pore size distribution provided is still a valuable graphic to have as it demonstrates our earlier observation that the panel glass had many more small pores while the funnel had a better size distribution. There are very large outliers for both compositions. Other composition results are not displayed here due to the datasets not being large enough for both the funnel and panel samples. These results could have been achieved more accurately through manual measurement techniques, however using a technique like this was preferred to show that it can be used on glass foams. A manual process is no use on a larger study with hundreds of samples and especially any type of manufacturing setting. This method, once perfected, could be implemented on a much larger scale due to its automated nature. The results could be improved through more image pre-processing and perfecting the code but the most apparent way to improve results would be to use pictures of a cut surface and not a fractured surface. A cut surface would provide the contrast difference needed for this process to consistently work.

B. Phase Identification

X-Ray diffraction was performed on the raw glass powder and the sintered samples so any formation of crystal phases during sintering could be observed.

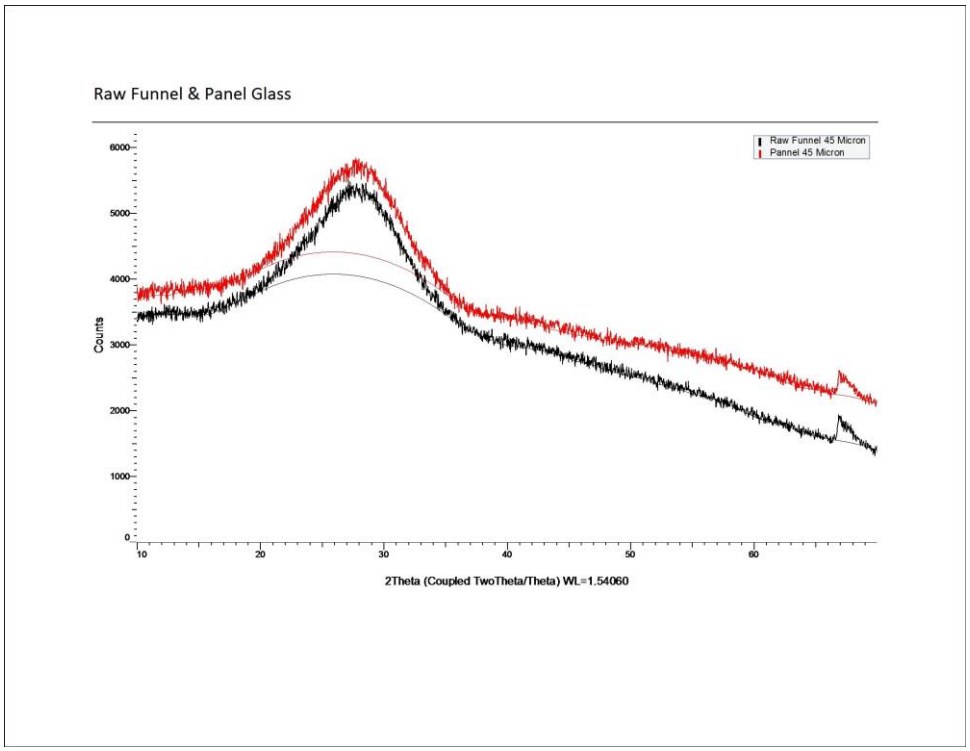

Figure 19. XRD patterns of both the raw panel and funnel glass

The XRD patterns shown above are of the cleaned raw panel and funnel glass. The patterns came back looking like a typical amorphous glass. These were ran just to show that the starting material was 100% amorphous. The XRD patterns were grouped into four images so that any spectra on the same graph shared foaming agent and glass composition. The PDFs inserted into the following spectra were placed as a comparison to the crystalline form of the metal oxides commonly found in the glass compositions. Not all of the PDF's matched to the spectra. They were inserted for comparison purposes and in most cases some amount was observed showing up in at least one composition.

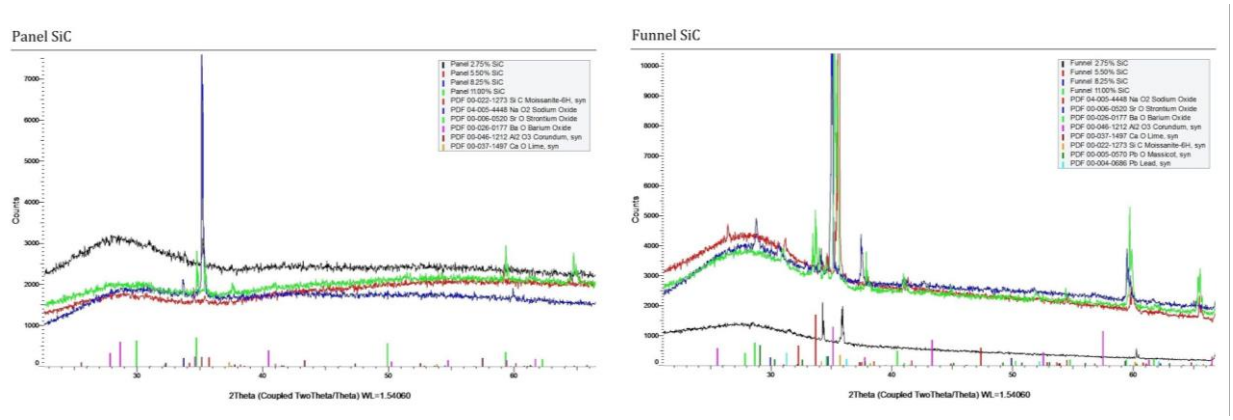

Figure 20. XRD patterns of both the raw panel and funnel glass foamed with SiC at all compositions

These spectra resemble the amorphous peak of the raw glasses but they also certainly have some prominent peaks. Firstly all spectra have a very prominent peak around 35(Two Theta) which is has been identified as the peak resulting from excess SiC in the structure that never got used up. This corresponds with our visual observations of the samples being darkened from higher compositions of SiC. For the panel spectra there are two other prominent peaks of interest. One of them is at 35 °2θ almost overlapped with the SiC peak and the other is just under 60 °2θ. At first observation both were thought to have been originated from crystallized Strontium and Barium or their oxides. Their spectra line up with those peaks, both of which contain 2 overlapping peaks. Unfortunately SrO and BaO are not easily reduced so it seems unlikely, but not impossible, that those peaks would belong to them. More research will have to be done to know what is exactly getting reduced from the Panel glass. For the funnel glass there are multiple peaks of interest especially over the Silica amorphous region. The peaks just to the left of the SiC peak are identified to be most likely from the lead getting reduced out of the glass and deposited in crystalline form. Some of the other peaks are thought to be caused by other present oxides from sodium and aluminum and possibly calcium. Even though barium and strontium are not present in the funnel in as high as weight percent they are still present and peaks are still observed where their spectra show up. More research will need to be conducted to discover if Sr and Ba are really being reduced from the glass or not.

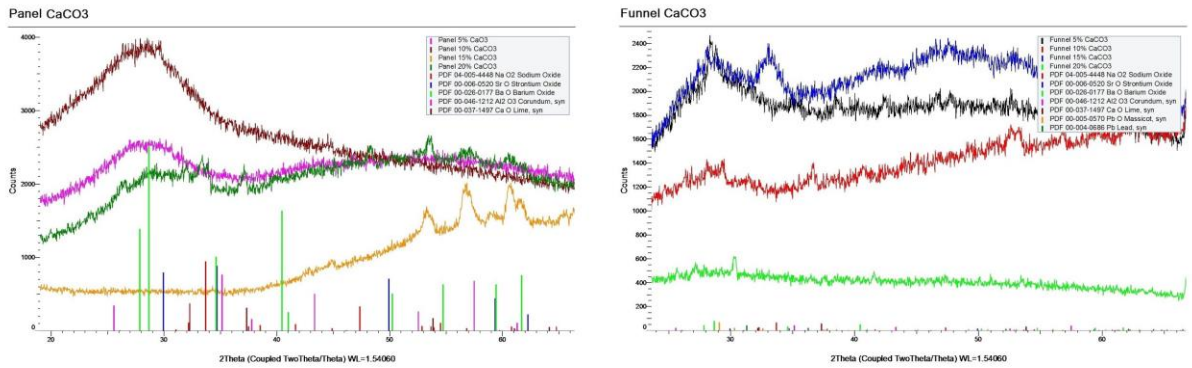

Figure 21. XRD patterns of both the raw panel and funnel glass foamed with CaCO3 at all compositions

The results for the panel and funnel glass showed a mostly amorphous XRD pattern. The panel glass, in particular, appeared to have peaks that corresponded to some of the metal oxides found in the CRT glass composition found in literature though in very small quantities. The presence of the peaks may suggest an oxidizing effect in the foams from using an extreme foaming temperature. The funnel glass had a greater amorphous structure throughout with minimal metal oxides, especially PbO and Pb crystals, present. Both panel and funnel XRD patterns showed small peaks for CaO, indicating that the thermal decomposition does leave traces of CaO as a byproduct. The hump over 20 to 35 °2θ range is typical of silica based glasses.

Compared to the XRD patterns from those found in literature the peaks are not apparent and were generally more amorphous. This is most likely caused from using the high sintering temperature. Literature searches yielded a max sintering temperature of 850 °C and usually held for shorter than 10 minutes (König et al. 2014). The cause for the peaks may be caused by the high temperature oxidizing the metal oxides but still in small enough quantities that it was not apparent in the SEM imaging. Using the solid sintered samples did not provide the clearest results and were mostly used as a qualitative measure to ensure that there were little to no oxidized crystals as was shown in the SiC samples. The 15 wt. % $CaCO_3$ sample that was used for the XRD analysis was very rough and had a small cross section, resulting in the missing hump from the 20 to 35 °2θ. The 20 wt. % sample also gave a very qualitative result due to the thin cross section.

C. Bulk & Skeletal Densities

The data shown in this section is the culmination of different density testing through pycnometry and Archimedes Method. The skeletal density is simply the density of the raw glass that the foam is made out of. The bulk density is the density of the foam including the gas it encloses within it. The raw densities outputted by the pycnometer for the raw funnel and panel glass were 3.0007 g/cm^3 and 2.7079 g/cm^3 respectively.

Table 2. Calculated densities from Pycnometry and Archimedes method for all samples

SiC	P 2.75%	P 5.5%	P 8.25%	P 11%	F 2.75%	F 5.5%	F 8.25%	F 11.00%
Bulk Density g/cm^3	2.0960	1.3197	1.2547	1.2605	0.8500	0.8231	0.6631	0.6306
Skeletal Density g/cm^3	2.2373	2.1690	2.4477	2.3849	2.2194	2.2895	2.3451	2.1782
Percent Porosity	6.3156	39.1546	48.7396	47.1466	61.7029	64.0484	71.7233	71.0475
$CaCO_3$	P 5%	P 10%	P 15%	P 20%	F 5%	F 10%	F 15%	F 20%
Bulk Density g/cm^3	0.1925	0.1940	0.2339	0.3757	0.1272	0.1712	0.2103	0.3297
Skeletal Density g/cm^3	2.2761	2.1021	2.2969	2.09F87	2.9629	2.9251	2.9250	2.7387
Percent Porosity	91.5420	90.7726	89.8177	82.0977	95.7078	94.1482	92.8091	87.9632

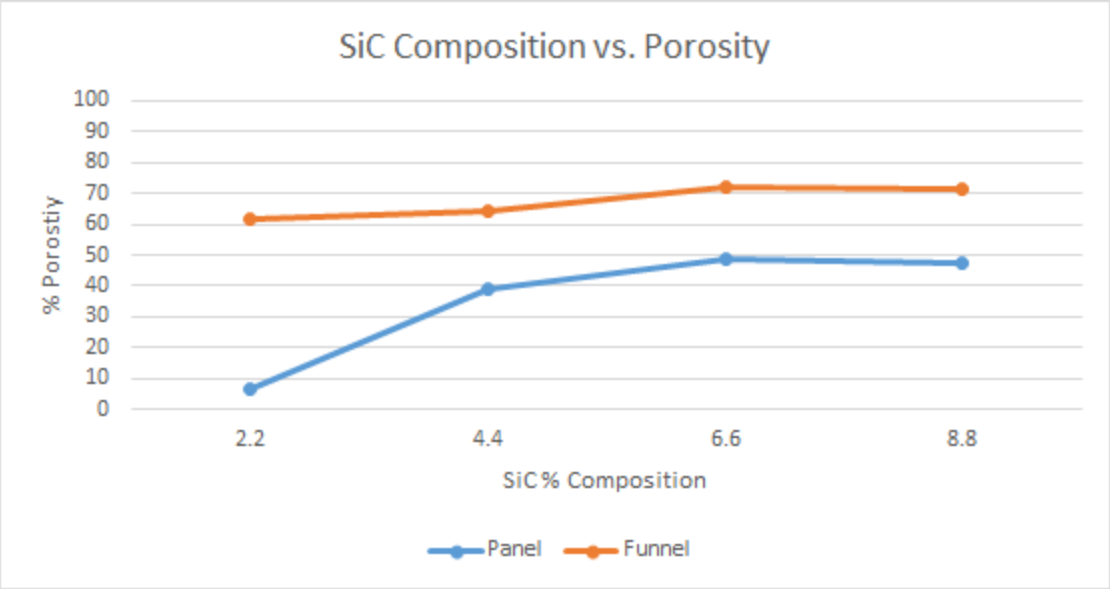

Figure 22. Graphed SiC composition vs. porosity for funnel and panel glass foams

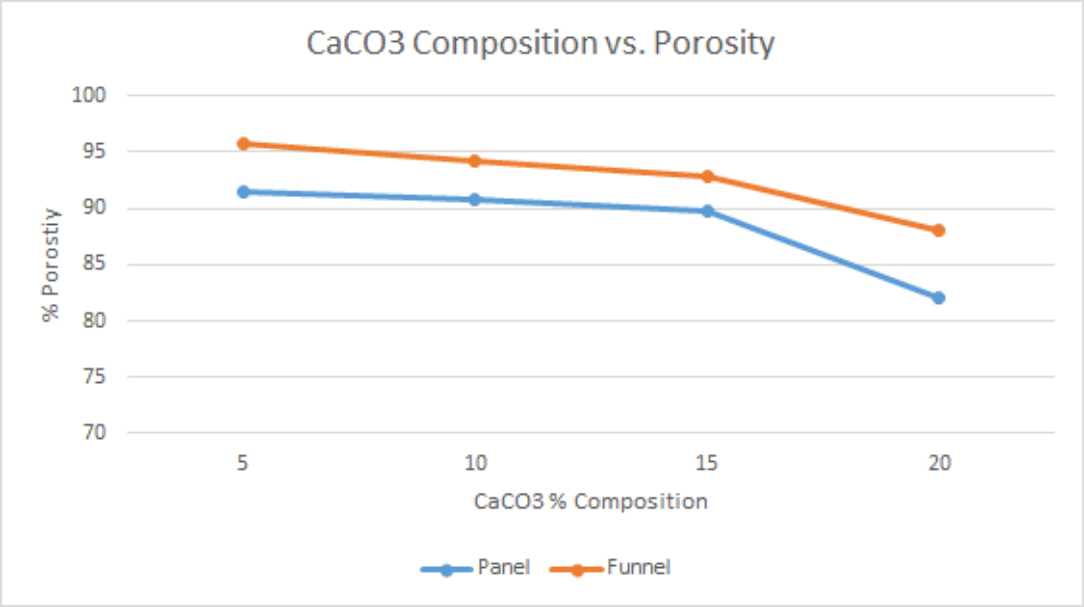

Figure 23. Graphed CaCO3 composition vs. porosity for funnel and panel glass foams

The graphs above help visualize the fact that the samples foamed more with SiC when the percent composition was increased and less with $CaCO_3$ when percent composition was increased. It should be noted that the particular change from 8.25% to 11% weight composition of SiC did not result in an increase in porosity for both panel and funnel glass and actually resulted in a slight decrease with both. Perhaps a saturation point of SiC in the glass has been reached but there would need to be more testing to conclude if that is or isn't actually the case.

These graphs help cement the idea that more foaming and lower bulk densities were achieved with the funnel glass than the panel glass. This could be caused by various things; there could have been something already in the pure funnel glass that would cause foaming on its own. A possibility could be an unknown coating on the funnel that could not be removed in preprocessing. Another possibility that could cause the funnel samples to foam more is that the funnel glass was likely softer at 900 C. This is due to the fact that there is less silica in funnel glass and more forms of other oxides. Panel glass averages 62% SiO_2 while Funnel glass only contains 52% SiO_2 on average *(Méar, 2006).* This final hypothesis is that the funnel glass foamed more is the fact that the funnel contains high amounts of PbO (19%–23%), a very easily reducible oxide. This could help explain why a larger relative increase in porosity was observed in the funnel glass with the SiC foaming over the $CaCO_3$ foaming.

IV. Conclusion

In this study, foam glasses were fast sintered (~600 s) successfully using a waste material (CRT glass) as the matrix. SiC and $CaCO_3$ were chosen as the two foaming agents to be used with SiC foaming the glass through a redox reaction and $CaCO_3$ foaming the glass through thermal decomposition. The structural and compositional characteristics of the foam glass samples were characterized to investigate the structural, processing, and composition relationship. The end product of this research presented a promising use of hazardous waste CRT glass and shed some light on the similarities and differences of two different foaming mechanisms.

The porous structure in the glass foams was found to be governed by the gas release rate. Produced reduction based foams showed potential to be used in applications such as shock-wave absorption, sound absorption, and heat retardation. Reduction based foaming also appeared to release portions of the heavy metal content from the glass. Methods of neutralizing these separated metals should be investigated so this waste glass can be safely recycled into glass foam products without risk to the environment and consumers. Glass foams using the thermal decomposition foaming method are able to produce more product on a volume basis and be applicable for sound absorption and heat retardation. Samples foamed using redox foaming method maintained a closed pore structure, and the bulk density decreased with increasing

addition of foaming agent; samples foamed by thermal decomposition method displayed open pore structures, and the bulk density increased with increasing addition of foaming agent. All foams made with funnel CRT glass have a lower bulk density compared to their panel glass counterparts.

More research is scheduled to be performed to experiment with methods of neutralizing heavy metals in the reduction based foams so that they could be used in the market without risk to consumers or the environment. Methods to create more uniform glass foams from $CaCO_3$ will also be investigated so that a stronger and more consistent product can be manufactured.

References

A.S. Apkaryan, S.N. Kulkov, and L.A. Gömze, "Foam Glass Ceramics as Composite Granulated Heat-Insulating Material,"*Epitoanyag - JSBCM Epitoanyag - Journal of Silicate Based and Composite Materials*, **66** [2] 38–42 (2014).

E. Bernardo, G. Scarinci, S. Hreglich, and G. Zangiacomi, "Effect of time and furnace atmosphere on the sintering of glasses from dismantled cathode ray tubes," *Journal of the European Ceramic Society*, **27** [2-3] 1637–1643 (2007).

E. Bernardo, R. Cedro, M. Florean, and S. Hreglich, "Reutilization and stabilization of wastes by the production of glass foams,"*Ceramics International*, **33** [6] 963–968 (2007).

E. Bernardo and F. Albertini, "Glass foams from dismantled cathode ray tubes," *Ceramics International*, **32**[6] 603–608 (2006).

H.R. Fernandes, D.D. Ferreira, F. Andreola, I. Lancellotti, L. Barbieri, and J.M. Ferreira, "Environmental friendly management of CRT glass by foaming with waste egg shells, calcite or dolomite," *Ceramics International*, **40** [8] 13371–13379 (2014).

Y. Gong, R. Dongol, C. Yatongchai, A. Wren, S. Sundaram, and N. Mellott, "Recycling of waste amber glass and porcine bone into fast sintered and high strength glass foams," *Journal of Cleaner Production*, **112** 4534–4539 (2016).

J. König, R.R. Petersen, and Y. Yue, "Fabrication of highly insulating foam glass made from CRT panel glass," *Ceramics International*, **41**[8] 9793–9800 (2015).

J. König, R.R. Petersen, and Y. Yue, “Influence of the glass–calcium carbonate mixture's characteristics on the foaming process and the properties of the foam glass,”*Journal of the European Ceramic Society*, **34** [6] 1591–1598 (2014).

S.W. Lee, S. Obregón-Alfaro, and V. Rodríguez-González, “Photocatalytic coatings of silver–TiO2 nanocomposites on foamed waste-glass prepared by sonochemical process,” *Journal of Photochemistry and Photobiology A: Chemistry*, **221** [1] 71–76 (2011)

N. Menad, “Cathode ray tube recycling,” *Resources, Conservation and Recycling*, **26** [3-4] 143–154 (1999).

C. Mugoni, M. Montorsi, C. Siligardi, F. Andreola, I. Lancellotti, E. Bernardo, and L. Barbieri, “Design of glass foams with low environmental impact,” *Ceramics International*, **41** [3] 3400–3408 (2015).

F. Méar, P. Yot, M. Cambon, and M. Ribes, “The characterization of waste cathode-ray tube glass,”*Waste Management*, **26** [12] 1468–1476 (2006).

F. Meyer, “Topographic distance and watershed lines,” *Signal Processing*, 38 [1] 113–125 (1994).

I. Nnorom, O. Osibanjo, and M. Ogwuegbu, “Global disposal strategies for waste cathode ray tubes,” *Resources, Conservation and Recycling*, **55** [3] 275–290 (2011).

C. Poon, “Management of CRT glass from discarded computer monitors and TV sets,” *Waste Management*, **28** [9] 1499 (2008).

M. Scheffler and P. Colombo,*Cellular ceramics: structure, manufacturing, properties and applications*. Wiley-VCH, Weinheim, 2005.

P.G. Yot and F.O. Méar, “Characterization of lead, barium and strontium leachability from foam glasses elaborated using waste cathode ray-tube glasses,” *Journal of Hazardous Materials*, **185** [1] 236–241 (2011).

Pittsburgh Corning USA , “FOAMGLAS ® INSULATION SYSTEMS,” (2009). http://www.insulation.org/mtl/pdfs/000256_494.pdf

Appendix

Solvent	Polyisocyanurate	Polyolefin	Polystyrene	Phenolic	FOAMGLAS® Insulation
Concentrated Nitric Acid	X			Dissolved	
Concentrated Hydrochloric Acid	X			X	
Concentrated Sulfuric Acid	Dissolved			X	
Concentrated Phosphoric Acid					
40% Nitric Acid	X			Dissolved	
10% Hydrochloric Acid	X				
30% Sulfuric Acid	X				
5% Carbolic Acid	X			X	
5% Acetic Acid	X	X		X	
10% Citric Acid	X	X			
Orange Terpenes		X	Dissolved		
Citrus Peel Oil		X	Dissolved		
Orange Juice	X	X		X	
Concentrated Ammonium Hydroxide	X	X		X	
Concentrated Potassium Hydroxide				X	X
10% Ammonium Hydroxide	X			X	
10% Sodium Hydroxide	X			X	X
2% Sodium Carbonate	X			X	
Heptane		X	X		
Methanol	X		X	X	
Formaldehyde	X			X	
Dichloromethane	X	X	Dissolved	X	
Benzene	X	X	Dissolved		
Methyl Ethyl Ketone	X	X	Dissolved	X	
1-Butanol	X			X	
Toluene	X	X	Dissolved		
Acetone	X	X	Dissolved	X	
Ethyl Acetate	X	X	Dissolved	X	
Mineral Spirits		X	Dissolved		
Ethylene Glycol		X		X	
Kerosene		X	Dissolved		

Appendix 1. Materials Which Showed Significant Changes in Volume and Weight When Immersed in Solvents (Pittsburg Corning)

CO_2 in $CaCO_3$	SiC with calculated amount of CO_2
$\frac{CaCO_3}{2g} = \frac{wt\%}{100\%}$	$\frac{C}{CO_2} = \frac{37.5\%}{100\%}$
$CaCO_3 = \frac{2g}{100\%} * wt\%$	$C = \frac{37.5\%}{100\%} * CO_2$
$\frac{CO_2}{CaCO_3} = \frac{44\%}{100\%}$	$\frac{C}{SiC} = \frac{30\%}{100\%}$
$CO_2 = \frac{44\%}{100\%} * CaCO_3$	$SiC = \frac{100\%}{30\%} * C$

Normalizing CO_2 Output in a 2 g sample

$CaCO_3$ wt. %	5.0000	10.0000	15.0000	20.0000
$CaCO_3$ (g)	0.1000	0.2000	0.3000	0.4000
98.5% Purity (g)	0.1015	0.2030	0.3045	0.4060
CO_2 (g)	0.0440	0.0880	0.1320	0.1760
CO_2 (g)	0.0440	0.0880	0.1320	0.1760
C (g)	0.0165	0.0330	0.0495	0.0660
SiC (g)	0.0550	0.1100	0.1650	0.2200
SiC wt %	2.7500	5.5000	8.2500	11.0000

Appendix 2. Calculation for 2g of foam glass with a normalized CO_2 output

Panel SiC

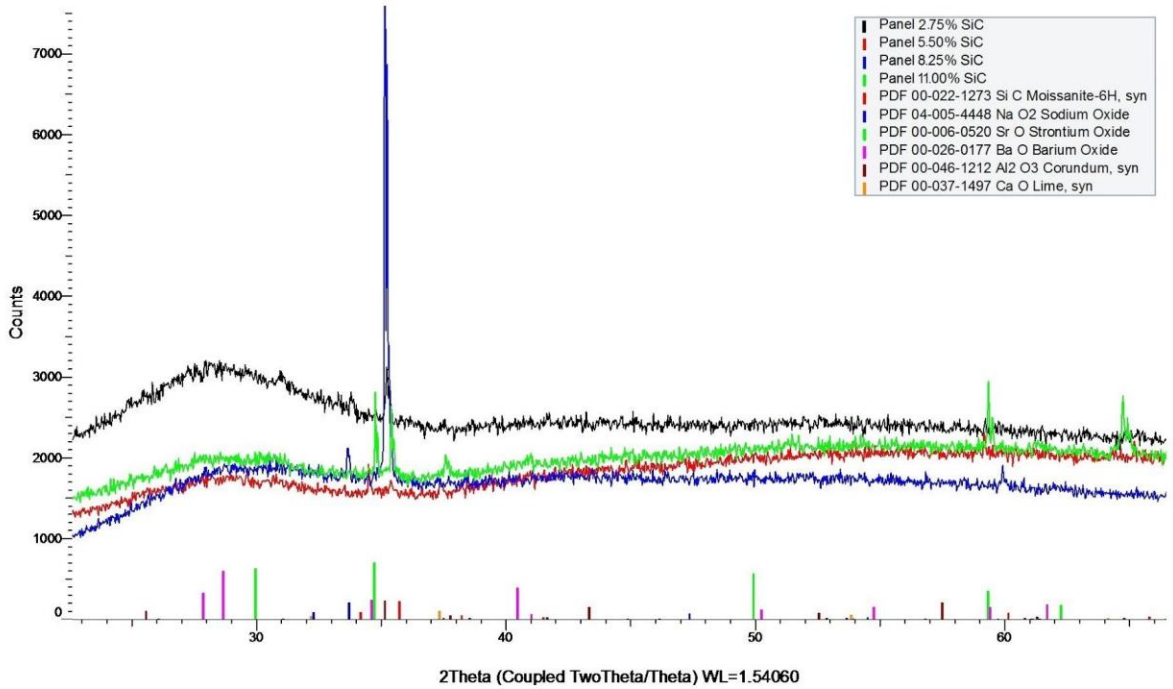

Funnel SiC

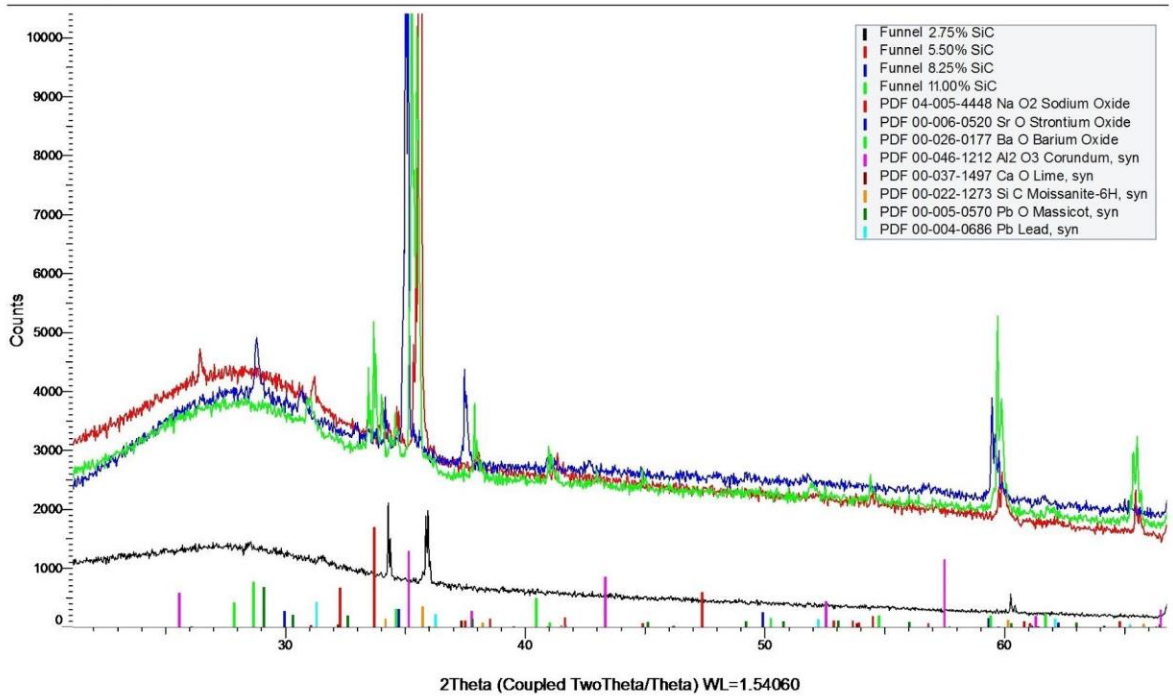

Appendix 3. XRD Patterns of SiC in Panel and Funnel Glass

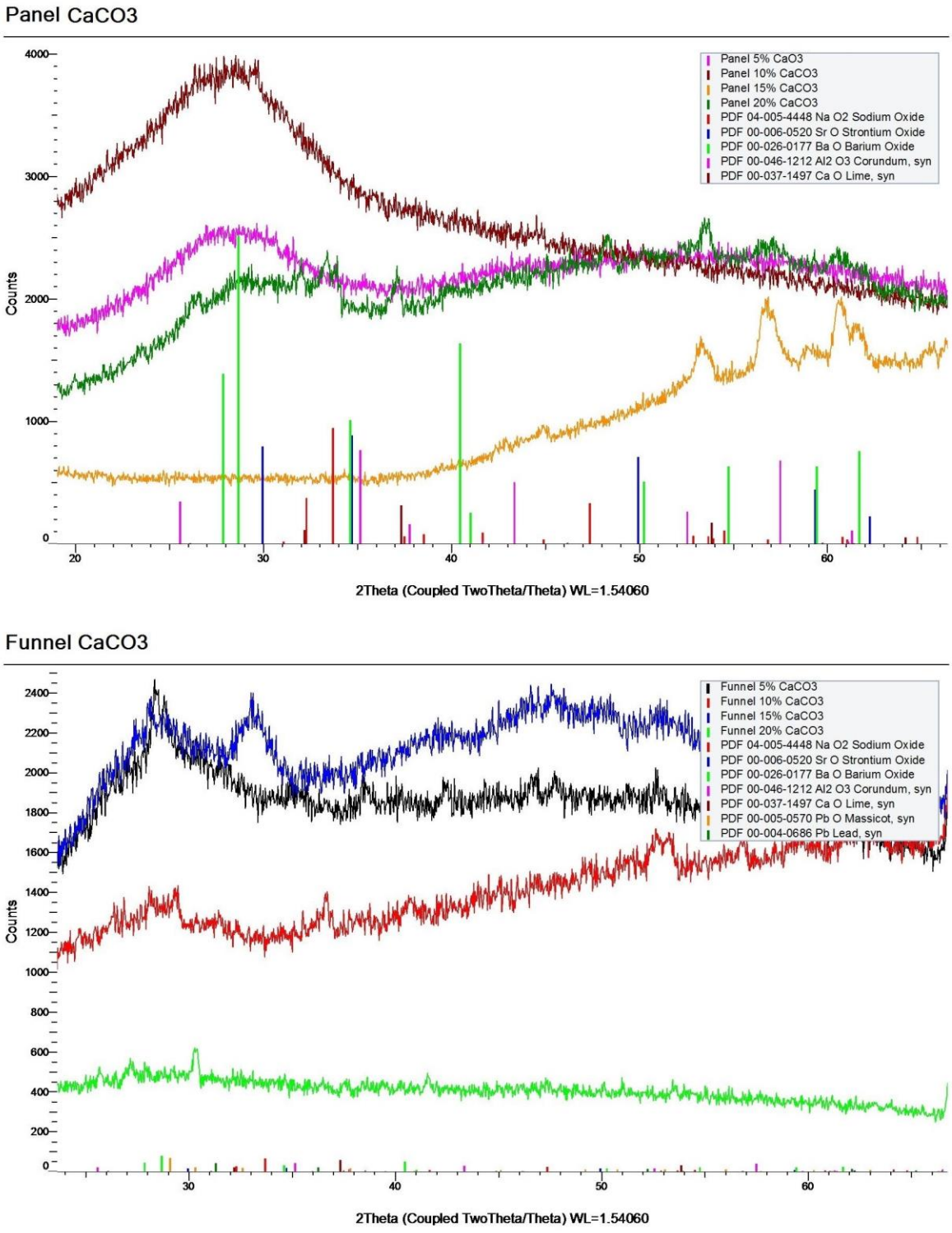

Appendix 4. XRD Patterns of $CaCO_3$ in Panel and Funnel Glass